2018 25th International Lightning Detection Conference &
7th International Lightning Meteorology Conference
March 12 - 15 | Ft. Lauderdale, Florida, USA

Broadband VHF Interferometry within the Kennedy Space Center Lightning Mapping Array

Mark A. Stanley, William Rison, Paul R. Krehbiel
Langmuir Laboratory
New Mexico Tech
Socorro, NM, USA
sparky@mark-stanley.name

Julia Tilles, Ningyu Liu
Space Science Center, Dept. of Physics
University of New Hampshire
Durham, NH, USA

Robert G. Brown, Jennifer Wilson
NASA Kennedy Space Center
Kennedy Space Center, FL, USA

***Abstract*—The New Mexico Tech broadband VHF interferometer was deployed at the Kennedy Space Center in 2016. A large number of narrow bipolar events were captured using a software triggering system based on a broadband VHF threshold. It will be shown that some of the narrow bipolar events were repeating in nearly the same location a few tenths of a second apart. Some of the events were composed of fast negative breakdown. The interferometer has also provided important insights into optical events detected by the Geostationary Lightning Mapper in 2017, including K-changes which are rarely detected unless they reach into the upper part of a storm.**

***Keywords*—VHF; NMT INTF; KSC LMA; NBE; K-change; GLM**

I. Introduction

The New Mexico Tech (NMT) broadband VHF interferometer (INTF) utilizes three 13” flat plate VHF antennas with a 3 dB bandwidth of 15-87 MHz. A fourth data channel records electric field data from a fast antenna. The system can record flashes in their entirety at a 180 MHz sample rate and 16-bit resolution, producing over 50,000 2D (azimuth, elevation) locations for a typical lightning flash [Stock et al., 2014]. This compares to roughly 1,000 3D locations for a typical flash by a Lightning Mapping Array (LMA) [Thomas et al., 2004].

The submicrosecond temporal resolution of the NMT INTF makes it ideal for mapping fast events such as narrow bipolar events (NBEs) and K-changes. NBEs produce some of the most energetic VHF radiation from lightning [Willett et al., 1989] and are known to be the initiating event of some lightning flashes [Rison et al., 1999]. NBEs observed by the NMT INTF at Langmuir Laboratory in 2013 were shown to be composed of fast positive breakdown with a propagation velocity in excess of 3×10^7 m/s [Rison et al., 2016].

K-changes are negative breakdown events which propagate back along prior positive leader channels towards and sometimes past the origin of an intracloud flash with velocities on the order of 10^6-10^7 m/s [Mazur and Ruhnke, 1993; Shao and Krehbiel, 1996]. Because they are energetic and can have significant horizontal extents, K-changes will likely be important to space-based optical lightning detectors such as the Geostationary Lightning Mapper (GLM) onboard GOES-16.

In this paper, we will show some select results from the field campaigns conducted in 2016 and 2017 with the NMT INTF situated near the center of the Kennedy Space Center (KSC) LMA.

II. Field Campaign

The NMT INTF was deployed at KSC on July 15, 2016. Aside from a multi-day power outage in early August of 2016, the system was operating continuously until hurricane Matthew visited KSC on October 7, 2016. The NMT INTF was repaired and redeployed at KSC on February 15, 2017. It operated continuously there until power was lost at the site on July 4, 2017.

The three VHF antennas were arranged in an equilateral triangle in 2016 with 100 meter baselines. A map of the site with antenna locations superimposed is shown in Fig. 1. The maximum useful mapping range of the system in 2016 was about 50 km.

This work was sponsored by NASA Grant Award 80NSSC18M000

Fig. 1: A satellite image map showing the 2017 VHF antennas (red), fast antenna (green) and slow antenna (magenta) locations. The 2016 VHF antenna locations are marked with hollow white diamonds while a temporary VHF antenna C location used only on February 15, 2017 is indicated by a hollow triangle. The INTF PC data acquisition system was located within the building with the checkerboard pattern top.

There were two primary modes of triggering which were often running simultaneously in 2016: one utilized a trigger signal output from a slow antenna to capture entire flashes while the other utilized broadband-threshold software triggering off of the raw VHF from one antenna. The software triggering was configured for much of 2016 to capture 105 ms duration records which were equally divided between pre- and post-trigger. Entire flashes could be captured by successive software triggers.

The VHF antennas could not be redeployed at the same locations in 2017 due to environmental cleanup activity at the site, but were instead deployed in a nearly right-triangle configuration with a longest baseline of 97 meters. The system was operated almost exclusively from VHF software triggering in 2017 with longer duration records in order to better capture entire flashes for comparison with GLM. The most common configuration was a 0.3/0.5 second pre/post trigger.

III. Narrow Bipolar Events

The Florida peninsula is host to a prolific number of NBEs during the summer months. There were likely well over a thousand NBE triggers which were within useful mapping range of the NMT INTF during 2016. In this section, we will highlight some interesting NBE behavior noted during the campaign.

A. Isolated Repeating Events

NBEs are typically defined to be isolated if they do not immediately precede (initiate) a flash or occur during one (rare). There were several storms for which a significant number of NBEs repeated within a localized volume with subsecond temporal separations, but did not initiate a flash. KSC LMA data is shown in Fig. 2 for a pair of NBE sequences which occurred within a 1.6 second interval starting at 01:14:55.6 UT on September 5, 2016. The parent storm was centered roughly 25 km to the east of the NMT INTF over the Atlantic.

The NMT INTF software triggered on all 5 NBEs shown in Fig. 2 as well as on the small IC flash within the core of the storm. Fig. 3 shows INTF azimuth/elevation data (round dots) for the triggers superimposed on LMA data (transparent diamonds) for a wider 3 minute interval centered on the events of interest. NBEs 1, 3 & 5 were all clustered together in the event at top left in Fig. 3 while NBEs 2 & 4 were clustered together in the event at top right. Both clusters are displaced a few kilometers above and to the left of the storm core in what appears to be an anvil.

Although the NBEs themselves are not well located by the LMA, the trailing weak sources on the negative breakdown end of the NBEs are well located and appear to be at 14-15 km altitude. These sources, which the INTF has shown to be common to all NBEs, generally persist for not much more than a millisecond.

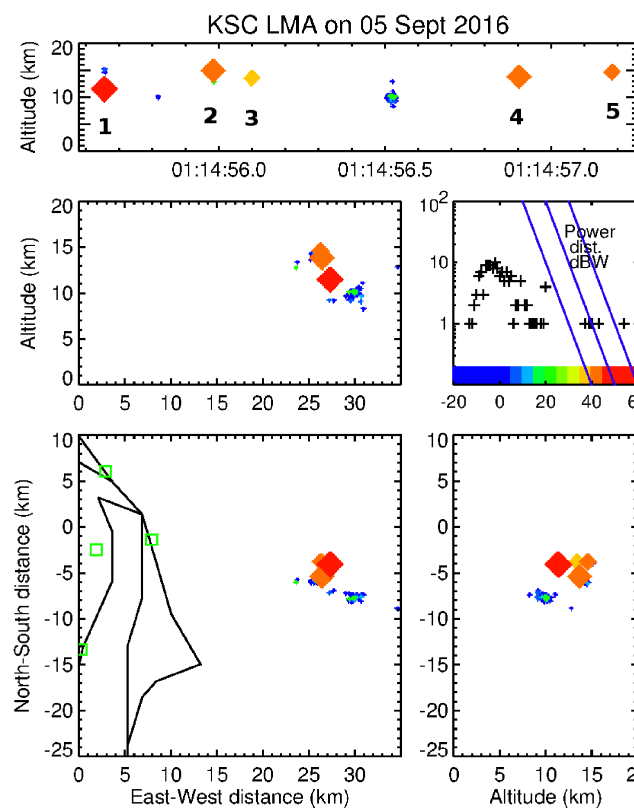

Fig. 2: There are 5 NBEs (orange-red diamonds) and one short duration IC flash (blue-cyan dot cluster) within this 1.6 second interval. LMA location errors mask the fact that NBEs 3-5 are alternating between the 2 locations where NBEs 1 & 2 initiated. The NBEs were about 24 km directly east of the NMT INTF at KSC.

and is consistent with each NBE at least partially discharging a high field region. Interestingly, the peak LMA VHF power of subsequent NBEs does not always follow this same trend (and is not necessarily expected to either).

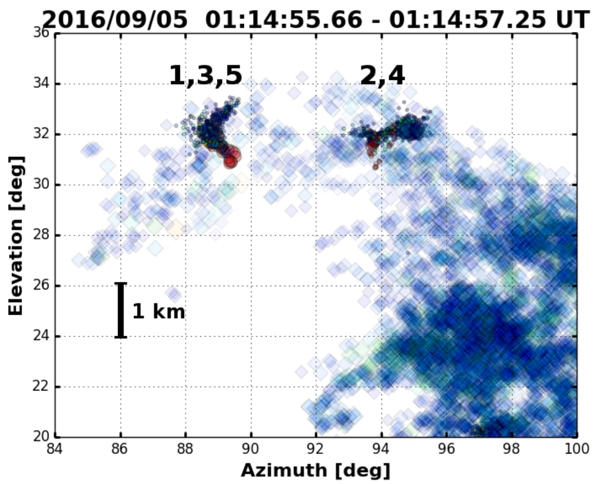

Fig. 3: INTF azimuth/elevation data for NBEs 1-5 is plotted with red colors and larger symbols corresponding to larger received VHF powers. NBEs 1, 3 & 5 all initiated within the same small region of the sky while NBEs 2 & 4 did so within a separate small region. The semi-transparent diamonds correspond to the apparent sky positions of 3D LMA sources within a 3 minute time interval centered on the NBEs. The convective core is clearly displaced to the right (south) of the NBEs.

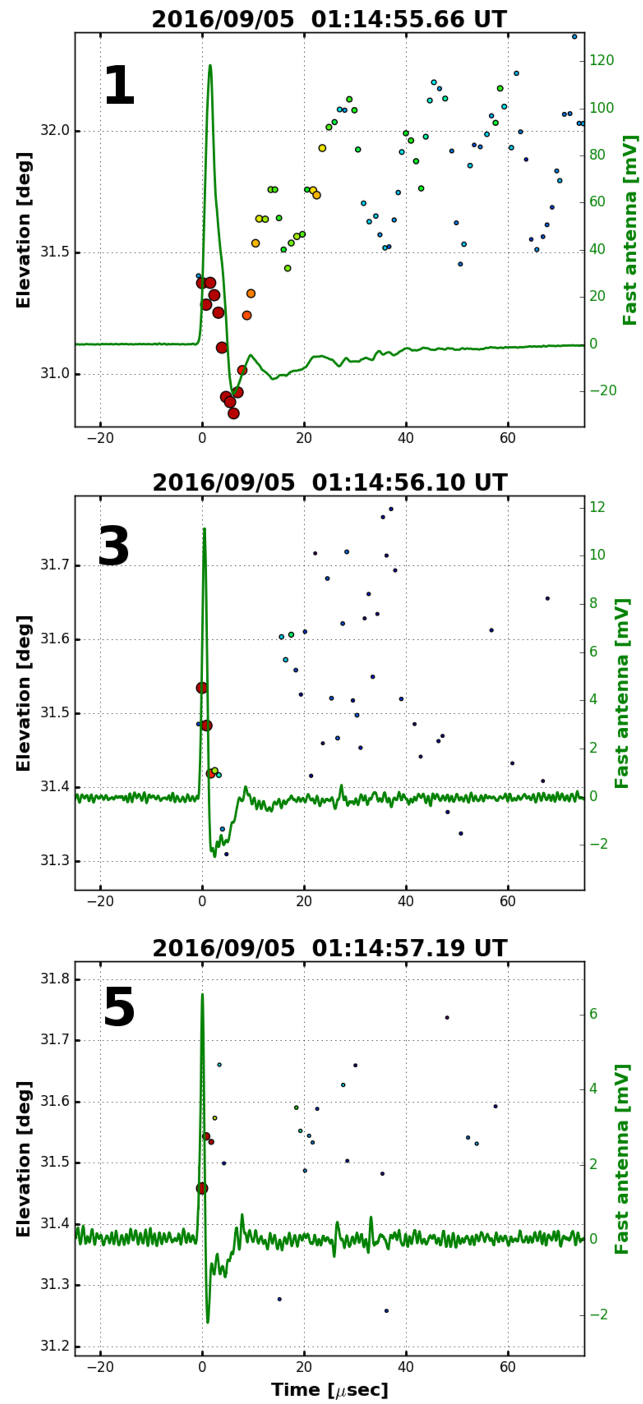

Fig. 4: The electric field waveforms of NBEs 1, 3 & 5 are shown with the elevation angle versus time development superimposed. As with the previous figure, larger dots correspond to larger received powers. The initial development of NBEs 1 & 3 is dominated by fast positive breakdown while the duration of NBE 5 is too short for motion to be resolved.

Fig. 4 shows a 100 microsecond zoom window of the NBEs 1, 3 & 5 with elevation versus time of INTF VHF sources plotted and the fast antenna electric field superimposed. In all cases the electric field deflection corresponds to the normal +NBE polarity in which negative charge is moving up (or, equivalently, positive down). Both NBEs 1 & 3 have initial fast positive breakdown, consistent with Rison et al [2016]. The NBE 5 duration is too short for motion to be resolved.

B. Fast Negative Breakdown

While not as common as fast positive breakdown, fast negative breakdown has also been observed in many NBEs [Tilles et al., 2017]. Fig. 6 shows that NBEs 2 & 4 were both dominated by fast negative breakdown. The elevation angle of the VHF sources in NBE 2 starts to decrease around 4 μsec post-onset and even drops below the initiation point before increasing again. One possible explanation for this is that both fast positive and fast negative breakdown are occurring simultaneously and that the former briefly becomes visible before vanishing as the latter declines in brightness.

The secondary electric field peaks which follow the NBE have been modeled as a bouncing wave phenomena on a transmission line [Hamlin et al., 2007, Nag and Rakov, 2010]. The fluctuation in the elevation angle of the VHF sources is not inconsistent with this explanation. However, Rison et al. [2016] showed from the analysis of close NBEs that the ripples likely arise from some other process. The source of the elevation angle fluctuations and ripples remains an area of active investigation.

One interesting thing to note in both Fig. 4 and Fig. 5 is that the amplitude and width of the fast antenna sferic for each subsequent NBEs is smaller than the one which preceded it. This has also been observed for other repeating NBE events

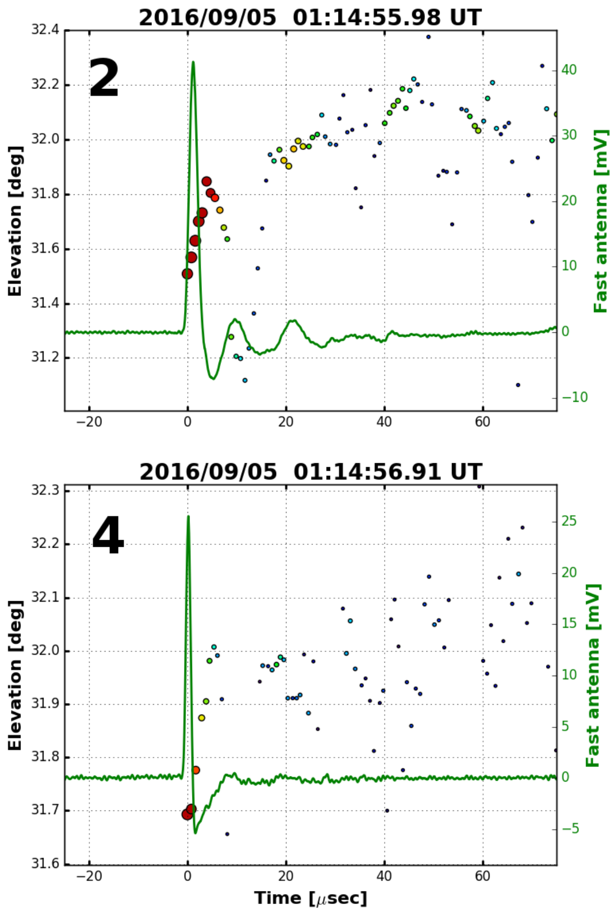

Fig. 5: NBEs 2 & 4 were dominated by fast negative breakdown. The sferic for NBE 2 was followed by ripples and the elevation angle of VHF sources also dipped briefly around the time of the first ripple.

IV. GLM Comparisons

A previous comparison of LMA data with that of NASA's Lightning Imaging Sensor (LIS) indicates that most detected optical events were associated with lightning channels that extended into the upper part of storms [Thomas et al, 2000]. In this section, a representative example will be shown of an altitude dependency for K-change optical detection.

Fig. 6 shows an INTF elevation angle versus time plot of a bilevel IC which occurred at 22:07:26 UT on May 1, 2017. The superimposed vertical magenta bars correspond to GLM optical detections from the flash with darker bars corresponding to multiple detections within a 2 ms window.

The burst of GLM detections over 100 milliseconds into the flash is associated with a second upward leader as it approaches the top of the cloud and propagates horizontally out in a different direction relative to the initial leader (which was not detected by GLM). The numerous vertical line segments in the plot correspond to K-changes. The only K-changes detected by GLM were those which propagated into the upper levels of the storm.

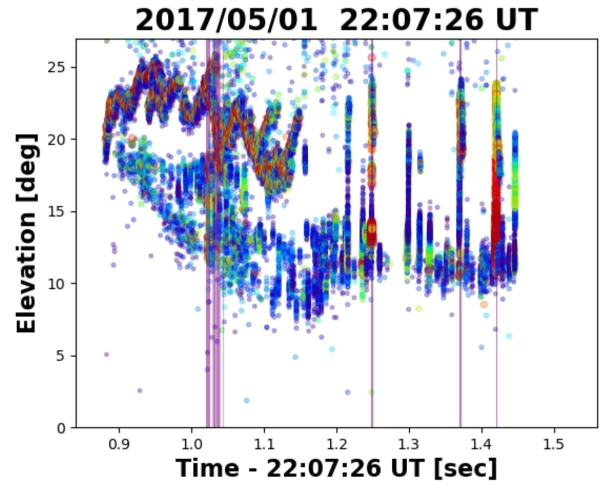

Fig. 6: The elevation angle of INTF VHF sources in this bilevel IC is plotted versus time with GLM optical detections superimposed as semi-transparent vertical magenta lines. The vertical line segments of VHF sources are all K-changes. Only some of those events which propagated into the upper levels were detected by GLM while all of those which remained in the lower level were not.

V. Discussion

The NMT INTF is an invaluable tool for mapping the progression of fast events and was highly complementary to the KSC LMA. Select examples were shown of repeating NBEs and fast negative breakdown which illustrate some of the rich variety of NBE behavior detected in Florida. In addition, the INTF is adding important insights into GLM detections which will lead to an improved understanding of the performance and limitations of satellite-based optical detectors.

Acknowledgment

We are indebted to Mike Stock's contributions to INTF post-processing software as well as the highly-effective broadband VHF software triggering algorithm. We thank Dan Rodenheffer for his assistance in setting up the INTF system as well as a pair of additional portable LMA stations at KSC. We are also grateful to the assistance of Levi Boggs in the INTF system deployment.

References

Hamlin, T., T. E. Light, X. M. Shao, K. B. Eack, and J. D. Harlin (2007), Estimating lightning channel characteristics of positive narrow bipolar events using intrachannel current reflection signatures, *J. Geophys. Res.*, *112*, D14108, doi:10.1029/2007JD008471.

Mazur, V. and L. H. Ruhnke, Common physical processes in natural and artificially triggered lightning, *J. Geophys. Res.*, *98*, 12,913-12,930, 1993.

Nag, A., and V. A. Rakov (2010), Compact intracloud lightning discharges: 1. Mechanism of electromagnetic radiation and modeling, *J. Geophys. Res.*, *115*, D20102, doi:10.1029/2010JD014235.

Rison, W., R. Thomas, P. Krehbiel, T. Hamlin and J. Harlin (1999), A GPS-based three-dimensional lightning mapping system, *Geophys. Res. Lett.*, *26*(23), 3573-3576.

Rison, W., P. R. Krehbiel, M. G. Stock, H. E. Edens, X. M. Shao, R. J. Thomas, M. A. Stanley and Y. Zhang (2016), Observations of narrow bipolar events reveal how lightning is initiated in thunderstorms, *Nat. Commun.*, *7*, doi:10.1038/ncomms10721.

Shao, X. M., and P. R. Krehbiel (1996), The spatial and temporal development of intracloud lightning, *J. Geophys. Res.*, *101*(D21), 26,641-26,668.

Stock, M. G., M. Akita, P. R. Krehbiel, W. Rison, H. E. Edens, Z. Kawasaki, and M. A. Stanley (2014), Continuous broadband digital interferometry of lightning using a generalized cross-correlation algorithm, *J. Geophys. Res. Atmos.*, *119*, 3134-3165, doi:10.1002/2013JD020217.

Thomas, R. J., P. R. Krehbiel, W. Rison, T. Hamlin, D. J. Boccippio, S. J. Goodman, and H. J. Christian (2000), Comparison of ground-based 3-dimensional lightning mapping observations with satellite based LIS observations in Oklahoma, *Geophys. Res. Lett.*, *27*(12), 1703-1706.

Thomas, R., P. Krehbiel, W. Rison, S. Hunyady, W. Winn, T. Hamlin and J. Harlin (2004), Accuracy of the lightning mapping array, *J. Geophys. Res.*, *109*, D14307, doi: 10.1029/2004JD004549.

Tilles, J., N. Y. Liu, P. R. Krehbiel, W. Rison, M. A. Stanley, R. G. Brown, J. G. Wilson, J. R. Dwyer, L. Boggs, and M. Stock (2017), Lightning narrow bipolar events produced by fast negative breakdown, *URSI General Assembly*, Montreal, Canada.

Willett, J. C., J. C. Bailey and E. P. Krider (1989), A class of unusual lightning electric field waveforms with very strong high-frequency radiation, *J. Geophys. Res.*, *94*, 16,255-16,267.